Environ. Sci. Technol. 1994, 28, 290–297

Mechanisms of Chromium(III) Sorption on Silica. 2. Effect of Reaction Conditions

Scott E. Fendorf*

Soil Science Division, University of Idaho, Moscow, Idaho 83844

Donald L. Sparks

Department of Plant and Soil Sciences, University of Delaware, Newark, Delaware 19717-1303

Metal ion retention on solids present in soils and waters decreases the risk of these contaminants as they are removed from the mobile aqueous phase. Determining the stability of the sorbed metal ions and the reaction conditions which influence the structure of the sorbate are necessary to evaluate the environmental risk of the sorbed moieties. In this study, a multitude of molecular level experimental techniques, including diffuse reflectance infrared Fourier transform (DRIFT) spectroscopy and high-resolution transmission electron microscopy (HRTEM), were employed to ascertain the Cr(III) surface structure on amorphous SiO_2 (silica) and reaction conditions (pH, solution Cr concentrations, and surface coverage) that affect the sorption mechanism. Chromium(III) formed a monodentate surface complex on silica at surface coverages less than 20%, while at greater surface coverages discrete chromium hydroxide surface clusters were discerned. Only the extent of surface coverage was observed to influence the atomic structure of Cr(III) on silica.

Introduction

Because of the agricultural, environmental, and industrial significance of metal retention reactions on oxides, it is important to obtain a detailed understanding of these reactions. Molecular level information is necessary to accurately deduce reaction mechanisms, which are essential for understanding chemical/physical factors affecting metal sorption/desorption processes. Although there is direct evidence for surface polymerization and nucleation of metal hydroxides (*1–8*), the reaction conditions affecting this process, e.g., pH, aqueous metal concentration, surface coverage (loading), and sorbent properties, are not clear. It is well-known that metal sorption is correlated with hydrolysis reactions of ions (*9*), which are primarily a function of pH. It remains unknown, however, whether this results primarily from surface complexation or metal hydroxide polymerization or precipitation. The extent of surface coverage necessary for nucleation (the initial point of a three-dimensional metal hydroxide growth) is also not apparent. The intent of this study was to investigate reaction factors influencing the Cr(III) sorption mechanism on silica.

A host of analytical techniques are available for investigating surface reactions, but no single technique is a panacea for obtaining mechanistic information. Rather, by using a combination of these techniques one can acquire an accurate and thorough depiction of interfacial reactions. Magnetic and vibration spectroscopies have been employed for investigating sorption reactions *in situ* without artifacts induced by the analytical conditions. While these spectroscopies provide important molecular level information, they do not always give a quantitative description of the local structural environment of a sorbed species. Nonetheless, they provide important information which can often be gained with less difficulty than with other techniques. X-ray absorption fine structure (XAFS) spectroscopy provides direct information on the local structure of sorbed (adsorbed or surface precipitated) metals.

Unfortunately, for reactions in soils and waters, *in situ* XAFS studies are limited to elements heavier than Sc, and synchrotron facilities necessary for *in situ* XAFS are usually not readily accessible. Furthermore, XAFS provides the local chemical environment of a particular element, but gives no information on the spatial resolution of surface species. In contrast to XAFS, transmission electron microscopy (TEM) provides information on the spatial resolution of surface modifications and the ordering (amorphous or degree of crystallinity) of the sorbed entities. Surface-probing microscopies (SPM) also offer spatial resolution, without subjecting a sample to electron bombardment, and give detailed atomic resolution information that is restricted to the surface. Vibrational spectroscopies provide information on the molecular aspects of the analyzed species.

Identifying surface structures is necessary to determine reaction mechanisms, to determine the stability of bound species, and for evaluating the physical/chemical properties of the modified surface. Therefore, the objective of this study was to investigate the surface structure of Cr(III) sorbed on SiO_2 and to determine the factors affecting the sorption mechanism—which ultimately influence the stability of the bound phase. By employing XAFS, diffuse reflectance infrared Fourier transform (DRIFT) spectroscopy, and high-resolution transmission electron microscopy (HRTEM), a multitude of atomic and molecular resolution information was obtained. This allowed for an accurate and detailed analysis of the Cr(III)–SiO_2 sorption mechanism. The local chemical and structural environment of Cr(III) was ascertained with the extended portion of XAFS, EXAFS (*10*), and molecular information with DRIFT. HRTEM provided spatial resolution and information on the surface structural modification of silica after reaction with Cr(III). One should recognize that in contrast to XAFS, both DRIFT and HRTEM are *ex situ* techniques in which the sample was exposed to 60 °C drying for the former and a vacuum environment for the latter. These techniques, nevertheless, do provide a useful characterization of the sorption mechanism, the data of which appear to correlate well with the results obtained from XAFS.

The DRIFT spectra were evaluated by comparing vibration modes of 'neat' silica, γ-CrOOH, and $MnSiO_3$ to

* To whom correspondence should be addressed.

0013-936X/94/0928-0290$04.50/0

the Cr–Si systems. The results gleaned from XAFS were compared to the information obtained with DRIFT analysis. This permitted the use of DRIFT for evaluating the effects of an extensive range of reaction parameters on the Cr(III) sorption structure.

Materials and Methods

Infrared Analysis. Diffuse reflectance infrared Fourier transform (DRIFT) spectroscopy was performed using a Perkins-Elmer FT-IR 1720X spectrometer with a diffuse reflectance accessory. Samples were prepared using the batch methods described previously (*10*). After reaction, the solid material was washed with 100 mL of deionized water, and the solids were dried at 60 °C for 24 h. The dried material was then diluted by 90% (by weight) with KBr to reduce the influences of spectral reflectance. Reported spectra are the average of 200 scans and are illustrated as the reflected intensity so that qualitative comparisons between spectra can be made.

In addition to the Cr–SiO_2 samples, reference materials were analyzed for comparison. Reference spectra were obtained for γ-CrOOH and SiO_2. The γ-CrOOH was a hydrous chromium oxide (HCO) precipitated by titrating 20 mM Cr(III) to pH 6, with pH maintained at this level for 24 h. This procedure was similar to that used by Charlet and Manceau (*2*). EXAFS analysis and electron diffraction patterns confirmed that the precipitated material was γ-CrOOH. The standards were also diluted by 90% (by weight) with KBr prior to DRIFT analysis.

HRTEM Analysis. High-resolution TEM was performed on high surface coverage Cr(III) reacted silica, ϕ = 9.9. For HRTEM analysis, 0.25 mL of the reacted suspension was dispersed on a holey carbon film supported by a fine mesh copper grid. The oxide-coated grids were then rinsed with 50 mL of deionized water and dried in a glass chamber. Imaging was performed on a Hitachi 9000NAR electron microscope. Further details on the electron microscopy procedures can be found elsewhere (*5*).

Cr(III) Concentration, Surface Area, and pH Effects. To evaluate the effect of the initial Cr(III) concentration and total surface area on the sorption mechanism, a systematic variance of each was conducted. The influence of initial metal concentration was investigated by keeping the total amount of Cr(III) (mol) and SiO_2 (g) constant while varying the solution volume. At pH 6, complete (100%) sorption of Cr(III) occurred at the initial concentration employed in this study. Thus, by keeping the quantity of SiO_2 (0.250 g) and Cr(III) constant (100 μmol) and varying the system's volume, a constant surface loading, ϕ = 0.20, under varying $[Cr]_o$ was obtained. Chromium(III) concentrations ranging from 40 μM to 1 mM were investigated. As in Fendorf et al. (*10*), data are referenced to the potential surface site occupancy, ϕ:

$$\phi = (\text{mol of Cr sorbed})/(\text{mol of surface sites}) \quad (1)$$

Again, one should be aware that this does not imply a site occupancy but only a potential maximum if each sorbed Cr(III) occupies a single site. If nucleation or precipitation occurs, then a different amount of the surface sites would be occupied (i.e., an amount less than ϕ would be covered). A reactive surface site density of 5.5 site/nm^2 (*11*) was used to calculate the site density for silica.

Surface coverage effects were evaluated by varying the amount of solid present while keeping $[Cr]_o$ and the volume constant. At low site occupancies (ϕ < 1), 2-L reactant systems having $[Cr]_o$ of 40, 100, and 200 μM were reacted with (i) 0.5 g of SiO_2 giving ϕ values of 0.079, 0.20, and 0.40, respectively, and (ii) 0.2 g of SiO_2 giving ϕ values of 0.22, 0.53, and 1.05, respectively. To determine the coverage effects at high surface loadings (ϕ > 1), 0.5, 1.0, and 1.5 g of SiO_2 were reacted with 5 mM $[Cr]_o$ in 2-L suspension volumes yielding surface coverages (ϕ) of 3.3, 5.0, and 9.9, respectively.

Table 1. Reaction Conditions Employed To Discern Effects of Reaction Parameters on Cr(III) Sorption Mechanism

varied reaction parameters	pH	$[Cr]_o$[a]	ϕ[b]	Γ[c]
pH	5.0	100	0.18	0.35
		200	0.25	0.50
		1000	0.33	0.64
	5.5	100	0.36	0.69
		200	0.57	1.1
		1000	0.86	1.7
	6.0	100	0.40	0.77
		200	0.79	1.6
		1000	1.6	3.1
surface coverage (ϕ < 1)	6.0	40	0.079	0.16
(0.25 g/L SiO_2)		100	0.20	0.39
		200	0.40	0.77
(0.1 g/L SiO_2)		40	0.21	0.40
		100	0.50	0.97
		200	0.99	1.9
(ϕ > 1)		5000	3.3	6.1
			4.9	9.0
			9.9	18
$[Cr]_o$ (varied suspension densities of SiO_2)	6.0	40	0.20	0.39
		400	0.20	0.39
		1000	0.20	0.39
$[Cr]_o$ and surface coverage	6.0	40	0.079	0.16
		100	0.20	0.39
		200	0.40	0.77
		5000	9.9	18

[a] Initial Cr(III)(aq), μM. [b] (mol of Cr)/(mol of surface sites). [c] (mol of Cr)/(g of SiO_2).

The effect of pH on the Cr(III) sorption mechanism was evaluated by investigating the reaction at pH values of 5.0, 5.5, and 6.0. These pH values correspond to approximately 20–24%, 45–55%, and 100% of the initial aqueous Cr(III) being sorbed on the silica (*10*). Table 1 summarizes the varied reaction parameters for these systems and provides pH, initial aqueous Cr(III) concentration, calculated potential surface site occupancy (ϕ), and measured quantity of Cr sorbed on the silica normalized to the mass of the sorbent (Γ = μmol of Cr sorbed/g of SiO_2).

Solution speciation imparts an important influence on metal sorption. Accordingly, the speciation of Cr(III) for each of the systems investigated is provided in Tables 2 and 3; the program MINTEQA2 (*12*) with the thermodynamic data of Rai et al. (*13*) was employed for the predicted speciation. The formation of polymeric Cr(III) species is unresolved. Rai et al. (*13*) reported that their data for pH values greater than 3.7 could not be explained considering polymeric Cr species. We have, however, provided the solution speciation of Cr(III), both considering polymeric species (Table 2) and restricting their formation (Table 3). The estimated thermodynamic values used for predicting the polymeric species are based on the highest possible stability constants if polymeric species dominate below pH 3.7 (*13*). Additionally, the saturation index (SI) with respect to $Cr(OH)_3 \cdot nH_2O$ is given in Tables 2 and 3 for the various reaction conditions studied.

Table 2. Speciation and Saturation Indices of Cr(III) Solutions Considering Polynuclear Species for Reaction Condition Employed[a]

species	pH	Cr(III) (μM)					
	5.0	50	100	200	400	1000	5000
Cr^{3+}			9.5	8.41	7.00	5.2	
$Cr(OH)^{2+}$			71.3	62.8	52.6	38.5	
$Cr(OH)_2^+$			1.8	1.6	1.30		
$Cr(OH)_3(aq)$							
$Cr_2(OH)_2^{4+}$			17.3	26.9	38	51.7	
$Cr_3(OH)_4^{5+}$						1.2	
$Cr_4(OH)_6^{6+}$						2.4	
SI			-0.112	0.133	0.356	0.616	
	5.5						
Cr^{3+}			3.02	2.7	2.2	1.5	
$Cr(OH)^{2+}$			72.3	62.9	51.3	34.7	
$Cr(OH)_2^+$			5.70	5.01	4.03	2.7	
$Cr(OH)_3(aq)$							
$Cr_2(OH)_2^{4+}$			17.8	27.1	36.1	42.1	
$Cr_3(OH)_4^{5+}$					1.3	2.7	
$Cr_4(OH)_6^{6+}$				1.3	4.7	16.2	
SI			0.894	1.13	1.35	1.57	
	6.0						
Cr^{3+}							
$Cr(OH)^{2+}$		68.1	62.7	53.6	41.1	24.8	8.00
$Cr(OH)_2^+$		17.0	15.6	13.4	10.2	6.10	1.91
$Cr(OH)_3(aq)$		5.71	5.31	4.5	3.4	2.11	
$Cr_2(OH)_2^{4+}$		7.94	13.4	19.6	23.2	21.5	12.4
$Cr_3(OH)_4^{5+}$				1.2	2.2	3.13	3.1
$Cr_4(OH)_6^{6+}$			1.6	6.9	19.3	42.1	73.8
SI		1.57	1.83	2.07	2.25	2.43	2.61

[a] Values were calculated using the speciation program MINTEQA-2 (*12*) with thermodynamic data from Rai et al. (*13*); polymeric proportions are the maximum based on the formation constants of Stünzi and Marty (*17*) and the solubility data of Rai et al. (*13*).

Table 3. Speciation and Saturation Indices of Cr(III) Solutions without Consideration of Polynuclear Species[a]

species	pH	Cr(III) (μM)					
	5.0	50	100	200	400	1000	5000
Cr^{3+}			11.5	11.5	11.5	11.6	
$Cr(OH)^{2+}$			86.3	86.3	86.3	86.2	
$Cr(OH)_2^+$			2.22	2.19	2.11	2.21	
$Cr(OH)_3(aq)$							
SI			-0.0291	0.271	0.571	0.967	
	5.5						
Cr^{3+}			3.7	3.7	3.7	3.8	
$Cr(OH)^{2+}$			88.5	88.5	88.5	88.6	
$Cr(OH)_2^+$			7.00	7.03	7.00	6.95	
$Cr(OH)_3(aq)$							
SI			0.982	1.28	1.58	1.98	
	6.0						
Cr^{3+}							
$Cr(OH)^{2+}$		74.2	74.2	74.3	74.3	74.3	74.7
$Cr(OH)_2^+$		18.5	18.5	18.5	18.5	18.5	18.2
$Cr(OH)_3(aq)$		6.21	6.21	6.2	6.21	6.2	6.1
SI		1.61	1.91	2.21	2.51	2.90	3.59

[a] Values were calculated using the speciation program MINTEQA2 (12) with thermodynamic data from Rai et al. (13).

Results

DRIFT Analysis. The DRIFT spectra for γ-CrOOH are shown in Figure 1. One notes a strong, sharp absorbance at 1385 cm^{-1} and a broader one at 1417 cm^{-1}. These peaks are characteristic of the bending modes for metal oxyhydroxides (Me–OH–Me) with the boehmite-type structure (γ-MeOOH) (*14*) and correlate well with the previously defined deformation modes of γ-CrOOH (*15*). The 1385-cm^{-1} peak is thus assigned to the in-plane (γ-OH) bending mode and the 1417 cm^{-1} peak to the out-of-plane (δ-OH) mode. The presence of these modes in the Cr–SiO_2 systems may be evidence for the formation of a γ-CrOOH precipitate or at least a moiety with a local structure similar to that of γ-CrOOH.

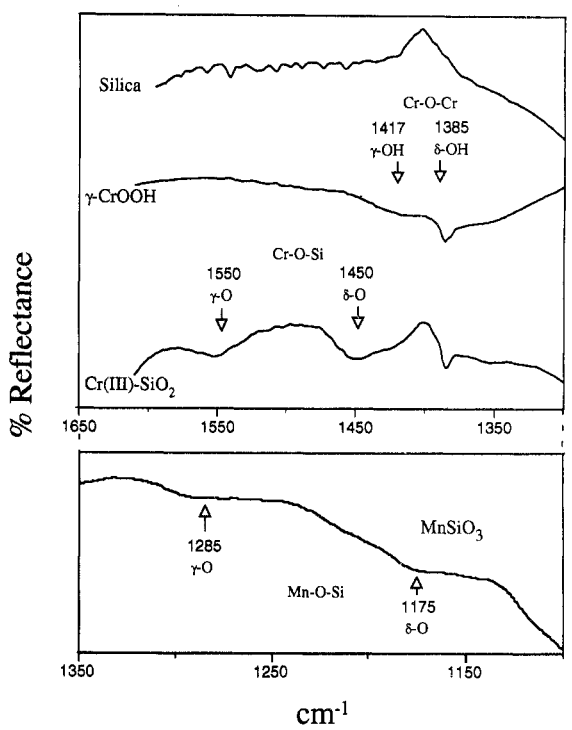

Figure 1. DRIFT spectra for silica, $Cr(OH)_3 \cdot nH_2O$, and $MnSiO_3$, and for Cr(III) sorbed on silica with ϕ = 9.9. The peaks at 1385 and 1417 cm^{-1} arise from the Cr–OH–Cr deformations, and the 1450- and 1550-cm^{-1} peaks are due to Cr–O–Si deformations.

The DRIFT spectrum of unreacted SiO_2 is also given in Figure 1. The 'neat' silica has a strong characteristic water vibrational band at 1630 cm^{-1}. However, the absorbance in the range of 1350–1600 cm^{-1} is minimal and, thus, does not interfere with the prominent bending modes of γ-CrOOH. Consequently, it appears that the 1385- and 1417-cm^{-1} bands in the Cr–SiO_2 spectra are good evidence for the formation of a multinuclear species with the γ-CrOOH structure, while their absence would suggest that surface polymerization or nucleation of this phase did not occur.

A third spectrum is shown in Figure 1: Cr(III) sorbed on silica (ϕ = 9.9). In this spectrum, 1385- and 1417-cm^{-1} peaks are visible, but additional absorbances at 1450 and 1550 cm^{-1} are also apparent. The 1385- and 1417-cm^{-1} absorbances are identical to those observed for the deformation modes in γ–CrOOH and, therefore, represent the formation of a multinuclear chromium hydroxide surface species with a local structure similar to γ–CrOOH. The 1450- and 1550-cm^{-1} peaks are not found in the chromium hydroxide spectra; their appearance and magnitude are correlated except under conditions where the 1450-cm^{-1} peak is obstructed by the 1417-cm^{-1} absorbance. These peaks may be representative of a Cr–O–Si interaction. The δ–O and γ-O bending modes in a monodentate Cr–O–Si bond should be shifted to higher energies than for Cr–OH–Cr (*14*). Consequently, the 1550-cm^{-1} peak is assigned to the δ–O vibration and the γ–O to the 1450-cm^{-1} vibration in a Cr–O–Si linkage. Furthermore, the Mn–O–Si in $MnSiO_3$ (rhodonite) is similar to the Cr–O–Si hypothesized complex (*16*), and consequently, their

Table 4. Assignment of Vibrational Modes for γ-CrOOH and Surface-Complexed Cr(III) on Silica

frequency (cm^{-1})	bond type	mode
1385	Cr–OH–Cr	γ-OH
1417	Cr–OH–Cr	δ-OH
1450	Cr–O–Si	γ-O
1550	Cr–O–Si	δ-O

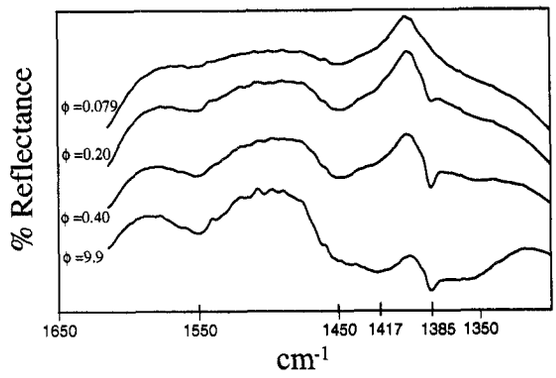

Figure 2. DRIFT spectra for Cr(III) sorbed on silica at $[Cr]_o$ of 40 (ϕ = 0.079), 100 (ϕ = 0.20), 200 (ϕ = 0.40), and 400 μM (ϕ = 0.79). The peaks at 1385 and 1417 cm^{-1} represent chromium hydroxide nucleation, while the absorbances at 1450 and 1550 cm^{-1} indicate a monodentate Cr–SiO2 complex.

vibrational modes should be similar. The Mn–O–Si δ–O and γ–O modes of $MnSiO_3$, however, should be shifted to lower energies than the Cr–O–Si modes; Figure 1 illustrates that indeed this was observed. Table 4 presents the assignment of the peaks for the DRIFT spectra of these materials.

With the assignment of the DRIFT peaks in the 1350–1600-cm^{-1} region, one can identify structural factors arising from the sorption of Cr(III) on silica. In addition, the ability to discern structural features in these systems with DRIFT can be determined.

DRIFT Analysis with Varying $[Cr]_o$ and Surface Coverage. The DRIFT spectra of 40, 100, 200, 400, and 5×10^3 μM $[Cr]_o$ resulting in ϕ values of 0.079, 0.20, 0.40, and 9.9, respectively, are presented in Figure 2. The latter four loadings were identical to those used in the XAFS study (*10*), permitting a comparison of results from these two techniques. With ϕ = 0.040 (20 μM $[Cr]_o$), no alteration from the unreacted SiO_2 spectrum was observed (data not shown). As ϕ increased to 0.079, relatively broad bands became apparent at 1450 and 1550 cm^{-1}. These broad bands increase in magnitude with further increases in ϕ and are the most prominent at the highest coverage (ϕ = 9.9) depicted in Figure 2. A sharp peak at 1385 cm^{-1} and a broader band at 1417 cm^{-1} are apparent at ϕ = 0.20 (100 μM $[Cr]_o$). The four peaks at 1385, 1417, 1450, and 1550 cm^{-1} all increase with continued increases in surface coverage, but the 1385- and 1417-cm^{-1} peaks clearly begin to dominate this spectral region at higher surface coverage. At ϕ = 9.9, the 1450-cm^{-1} mode becomes only a poorly resolved shoulder on the 1417-cm^{-1} absorbance.

At ϕ = 0.040 (20 μM $[Cr]_o$), no structural modifications are apparent from the DRIFT spectra (not shown). However, with a 2-fold increase in coverage, ϕ = 0.079, the monodentate surface complex (Cr–O–Si) was observed; thus, the detection for sorbed Cr on silica was between ϕ = 0.040 and 0.079. The 0.079 coverage spectra do not indicate the presence of polymerized or nucleated chromium hydroxide species. A surface structure with spectral features like γ-CrOOH is discerned at a potential site coverage of 0.20, as noted by the 1385- and 1417-cm^{-1} absorbances. Hence, DRIFT spectra indicate that the limits of measurement for Cr–O–Si in this experiment reside at ϕ less than 0.079, that monodentate surface complexation of Cr on silica occurs at ϕ < 0.20 (100 μM $[Cr]_o$), and that a surface phase with a local structure similar to γ-CrOOH becomes detectable at $\phi \geq 0.20$. These values represent structures derived with DRIFT in our studies; monodentate complexation and polymerization probably begin at lower surface coverages but were not discernible. Additionally, other surface structures of Cr(III) may be present in undetectable quantities. The DRIFT spectra therefore may be viewed as gleaning information on the dominant surface structures present in these systems.

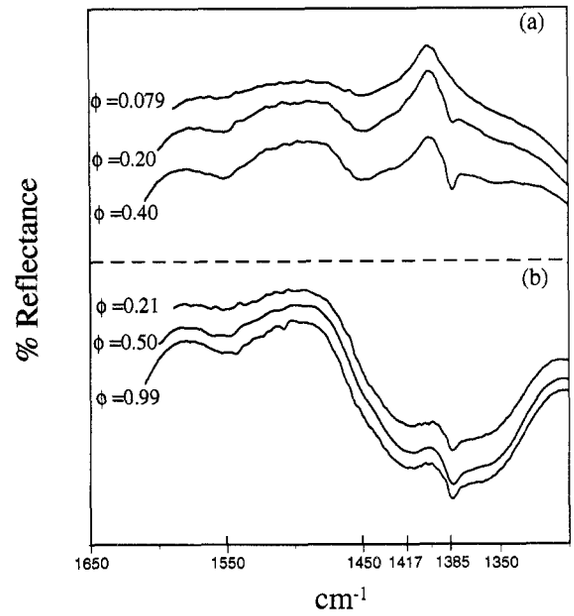

Figure 3. Effects of surface coverage at less than potential monolayer coverage (ϕ <1). Initial Cr(III) concentrations of 40, 100, and 200 μM were reacted with (a) 0.5 g of SiO_2 and (b) 0.2 g of SiO.

Initial Cr(III) Concentration and Surface Coverage Effects. A second set of reaction systems was investigated in which the initial Cr(III) concentration was varied from 40 to 800 μM while the surface loading remained constant. A potential site occupancy (ϕ) of 0.20 was employed in these systems, which would not require nucleation for complete Cr(III) sorption. This allowed for an assessment of $[Cr]_o$ effects on the Cr(III) surface structure. Under these reaction conditions, no appreciable alteration in the DRIFT spectra was detected (data not shown). Absorption bands characteristic of Cr(III) complexed on silica were apparent, with no indication of multinuclear chromium hydroxide surface species. Therefore, at low surface coverage, the sorption mechanism is affected by ϕ while not being influenced by $[Cr]_o$.

The degree of surface coverage was varied by investigating two oxide quantities while maintaining $[Cr]_o$ constant. At less than monolayer coverage, the extent of surface coverage on the Cr(III) surface structure was dramatic, as illustrated in Figure 3. Under equal $[Cr]_o$, a potential site coverage of 0.079 resulted in the formation of a monodentate Cr(III) surface complex (top spectrum, Figure 3a), as indicated by the absorbances at 1450 and 1550 cm^{-1}, while a ϕ of 0.21 gave evidence for a surface

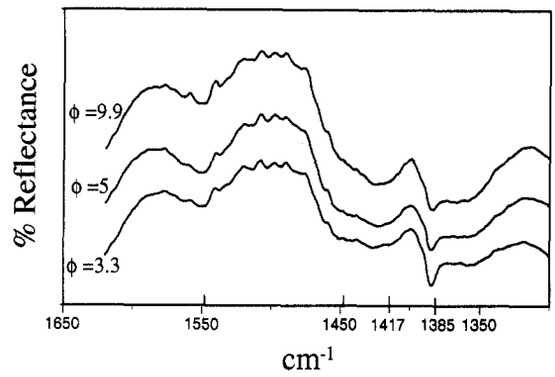

Figure 4. Surface coverage effects at greater than monolayer coverage. An initial Cr(III) concentration of 5 mM was reacted with 0.5 g (ϕ = 9.9), 1.0 g (ϕ = 5.0), and 1.5 g (ϕ = 3.3) of SiO_2.

phase with the γ-CrOOH local structure (top spectrum, Figure 3b). The effects of surface coverage, at fractional coverage, are further exemplified by the different coverages investigated (Figure 3). In Figure 3a, an increase in ϕ from 0.079 to 0.40 resulted in increasing intensities and the prominence of the 1450- and 1550-cm^{-1} bands, with the 1385- and 1417-cm^{-1} bands becoming apparent at a ϕ of 0.20. This indicates that monodentate Cr(III) surface complexation on silica predominates at a ϕ of 0.079–0.20, but polymerization, and possibly nucleation, of a γ-CrOOH-type surface species occurs at ϕ values greater than 0.20 and increases at higher coverages.

With potential site occupancies greater than 1, the surface structure is not influenced by varying ϕ. This is illustrated in Figure 4 in which varying amounts of silica were reacted with equal $[Cr]_o$. In these systems, extensive nucleation was noted with very little difference in the DRIFT spectra for ϕ ranging from 3.3 to 9.9.

pH and Solution Speciation Effects. Three pH values were investigated to determine the influence of solution pH on the sorption mechanism. However, one should note that pH effects on the surface structure probably arise solely from changes in the surface coverage, which is a function of the pH. Figure 5 presents the DRIFT spectra of Cr(III) sorbed on silica at pH 5.0, 5.5, and 6.0. At pH 5, very little surface complexation of Cr(III) is observed from the DRIFT spectra (viz., the absence of the 1450- and 1550-cm^{-1} modes). As pH increased to 5.5, more extensive sorption occurs and the Cr–O–Si bond becomes apparent; in addition, γ-CrOOH-type absorbances are observed (viz., 1417- and 1385-cm^{-1} absorbances). The pH 6 spectra are dominated by absorbances characteristic of γ-CrOOH.

The DRIFT spectra of similar ϕ values correspond well with each other (i.e., a surface loading of ϕ is similar whether the reaction occurred at pH 5, 5.5, or 6). It appears that pH has little direct impact on the surface structure, but plays a major role by influencing the extent of sorption. Therefore, the predominant role of pH is in determining the amount of sorption, which does affect the surface structure.

The similarity in the spectra of comparable surface loadings that were derived from different solution conditions also indicates that changes in solution speciation did not influence the sorbed structure. Solution speciation clearly influences the amount of sorption but does not appear to influence the resulting Cr(III) surface structure. Monomeric speciation seems more consistent with the sorption data than polymeric solution speciation. This is

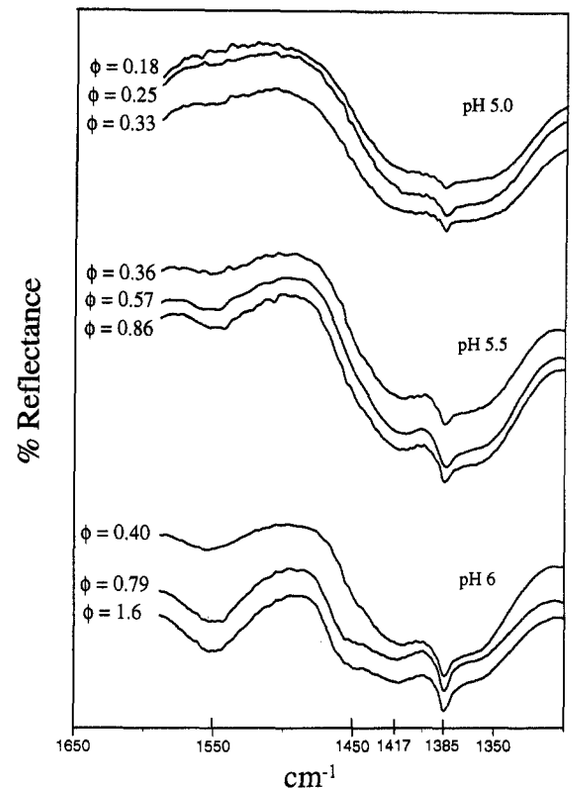

Figure 5. DRIFT spectra of Cr(III) sorbed on silica at pH 5.0, 5.5, and 6.0 with 100, 200, and 1000 μM $[Cr]_o$, respectively.

illustrated by the greater amount of polymeric species (Table 2) predicted at pH 5 and 1000 μM Cr(III) than at pH 6 and 100 μM Cr(III), but a greater amount of sorption occurring with the latter conditions (Γ = 0.35 for the former and 0.77 for the latter, Table 1). As a consequence, either the presence of polymeric solution species does not influence the extent of sorption appreciable, which does not seem reasonable based on their charge, or the predicted values are incorrect. The solution speciation of Rai et al. (*13*) also indicated the absence of polymeric species over a similar pH range.

Spatiality of Nucleation Growth. Although both EXAFS and DRIFT data give important information on the local structural environment of Cr(III), it is difficult to determine the spatial proximity and long-range order of the sorbed material with these two methods. Accordingly, HRTEM was employed to deduce further structural information.

Imaging was performed prior to and after reaction with Cr(III), ϕ = 9.9 (Figure 6). The silica was completely amorphous, showing no indications of ordering (marked A in Figure 6). After reaction with Cr(III), distinct crystalline areas approximately 20 × 20 nm are clearly visible (marked B in Figure 6). The crystalline areas are γ-CrOOH surface clusters. The HRTEM images reveal that even when there was greater than 10 times the amount of Cr necessary to occupy all the reactive surface sites, discrete crystalline particles formed. Since surface features must have a depth dimension in order to be observed with TEM, we cannot exclude the possibility of monomer or small polymeric Cr(III) species being present on the silica surface. However, the electron micrograph does indicate that chromium hydroxide nucleation did not progress over the silica surface but rather formed isolated nucleated areas (island structures) which, at least with

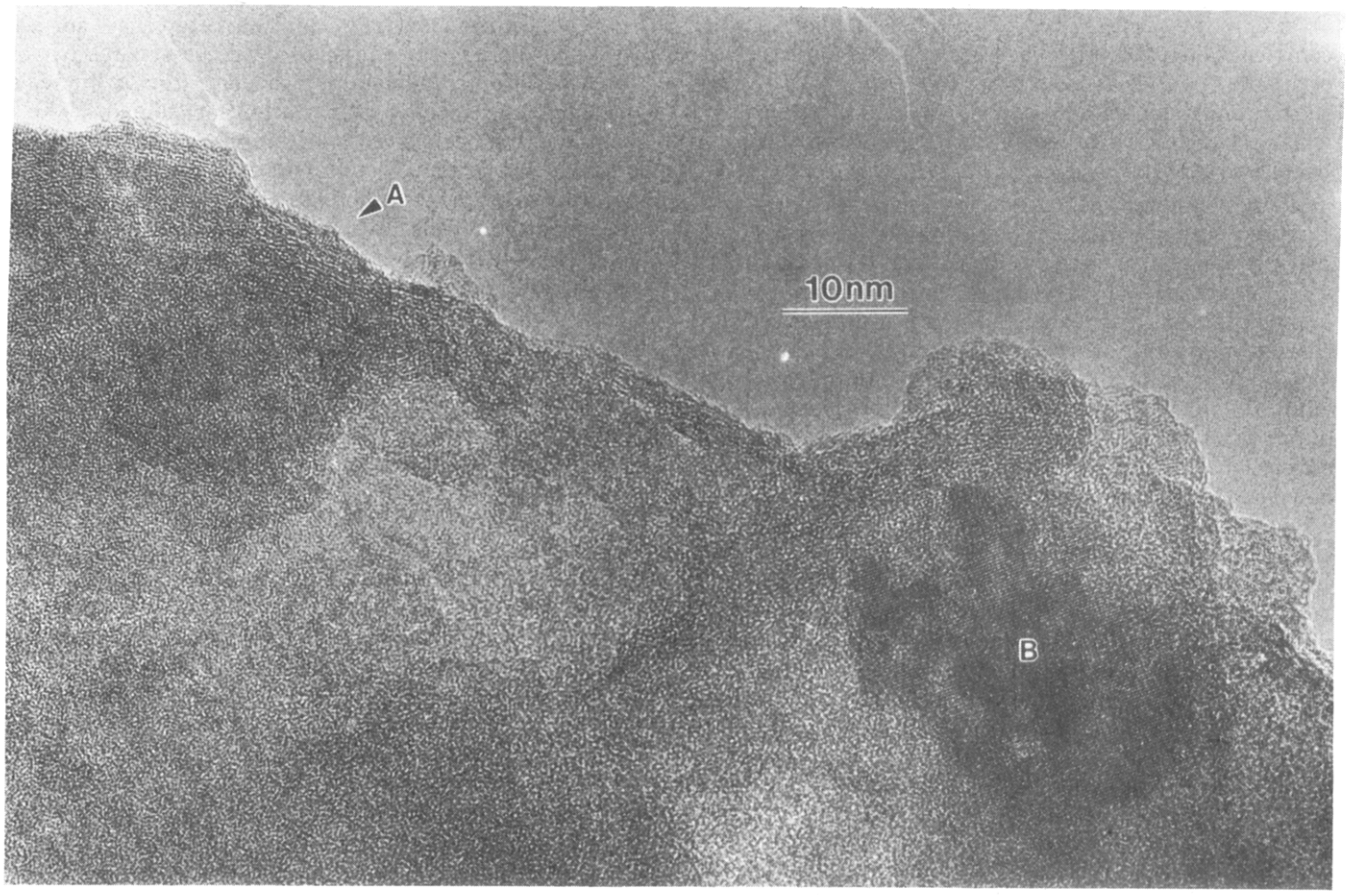

Figure 6. High-resolution TEM image of silica after reaction with 5 μM Cr(III) at pH 6 (ϕ = 9.9). A discrete crystalline γ-CrOOH surface precipitate (marked B) has formed on the amorphous silica (marked A).

high potential surface coverage, possessed relatively long-range order (crystallinity).

Discussion

Both EXAFS (*10*) and DRIFT analyses indicate that Cr(III) formed an inner-sphere monodentate surface complex on silica. At potential site occupancies (ϕ) below 0.20, only Cr(III) complexed with silica was observed. At coverages equal to and exceeding 0.20, a surface phase with the γ-CrOOH-type structure was observed. At ϕ = 9.9, surface clusters with the γ-CrOOH-type structure were clearly distinguishable. A progression from isolated site binding at low coverages to surface hydroxide nucleation of Cu^{2+} on aluminum oxides was similarly observed (*7*, *8*).

Chromium(III) sorption on α-FeOOH results in a surface precipitate with the α-CrOOH-type structure (*2*); as surface coverage increased, polymerization expanded over the surface before expanding outward (away from the surface). Further increases in Cr(III) quantities resulted in nucleation that progressed outward from the α-FeOOH surface. Additionally, there was a phase transition to the γ-CrOOH-type structure (*2*). Our results indicate that various phenomena also contribute to the sorption of Cr(III) on silica. A monodentate complex of Cr(III) on silica forms; the complexation continues but polymerization of a γ-CrOOH-type phase occurs well before monolayer coverage. With a continued increase in Cr(III) levels (ϕ > 0.20), polymerization progressed on the silica surface as noted by increases in Cr–O–Si and Cr–OH–Cr modes (viz., DRIFT spectra). Further increases in coverage resulted in nucleation and the dominance of a 'relaxed' γ-CrOOH precipitate as evident by the Cr–OH–Cr modes occurring at the same frequency as those of the homogeneous HCO precipitate. High-resolution TEM indicated the formation of a γ-CrOOH structure, which formed discrete particles, surface clusters, on the silica surface even when greater than near 10 times monolayer coverage was possible (ϕ = 9.9).

Reaction Factors Influencing the Sorption Mechanism. Various reaction factors may influence the sorption mechanism: pH, metal concentration, surface coverage, and sorbent type. In this study, we evaluated how these four factors affected the surface structure of Cr(III) sorbed on silica. It is well-known that pH and metal concentrations affect the extent of metal sorption. Moreover, the correlation between hydrolysis reactions and the sorption of cationic metals is also well established (*9*). The extent of surface coverage and sorbent type also influence sorption, but in a less defined manner. The influences of these parameters on the sorption mechanism and resulting surface structure are not resolved.

In this study, various atomic level experimental techniques were employed over a range of reaction conditions to help clarify the phenomena governing the sorption mechanism. Our findings indicate that solution metal concentrations and pH indirectly influence the sorption structure of Cr(III) on silica by determining the extent of sorption. The dominant reaction factor influencing the sorption mechanism is the degree of surface coverage.

Isolated site adsorption was discerned only at site occupancies less than 20% (ϕ < 0.20). At higher surface coverages, nucleation of HCO (γ-CrOOH local structure) occurred. Thus, it appears that it is more energetically

favorable for surface hydroxide nucleation than for complexation of Cr(III) on silica when a surface site occupancy of 20% is exceeded. Furthermore, the precipitate does not grow across the silica surface, but instead forms crystalline clustered (island) structures that protrude away from the surface.

In this system, the correlation between hydrolysis reactions and sorption may be dominated by surface precipitation rather than by adsorption. If one views the surface complexation reaction as a similar phenomenon to precipitation (i.e., the central cation tries to adopt the coordination environment of lowest energy), after a hydrolysis reaction Cr(III) would bind to the surface and enter a more favorable coordination environment. The hydrolysis reaction disrupts the symmetric hexaqua coordination of a metal. This results in a less stable structure in which the H_2O group opposite the OH moiety becomes a 'good' leaving group and, thus, promotes metal ion adsorption and/or nucleation. As adsorption increases, Cr would continue to bind at isolated sites, but would begin to bridge together with O or OH species to further satisfy its coordination shell (polymerization). On a surface such as α-FeOOH, where the structural environment is similar to that for chromium hydroxides, polymerization progresses over the surface—epitaxial growth (2). Once a monolayer of coverage has occurred, nucleation must occur and progress outward from the surface. At some distance from the Fe surface, a phase transition to the homogeneous precipitate structure (γ-CrOOH) occurred (2). However, for Cr(III) sorption on silica, polymerization cannot progress across the silica surface due to differences in the interatomic distances of silica versus chromium hydroxide; thus, epitaxial growth is inhibited. Consequently, nucleation occurs and progresses away from the surface to satisfy the coordination environment of the Cr.

The electrostatic influences of a charged surface clearly can catalyze precipitation, as exemplified by chromium hydroxide surface precipitation on δ-MnO_2 (2, 5). However, complexation on an oxide can also promote, or at least be the precursor to, the nucleation of the metal hydroxide. Complexation-promoted nucleation imparts a structural influence from the sorbent on the nucleation structure. For nucleation on structures with favorable parameters (interatomic site distances), epitaxial-type growth occurs until a distance is reached from the sorbent/precipitate interface where the structure of the homogeneous precipitate is adopted. This scenario is observed for chromium hydroxide nucleation on goethite (2). When the structural constraints of the sorbent are not favorable for epitaxial growth, nucleation proceeds in discrete clusters which develop away from the surface rather than across it. This was observed for Cr(III) sorption on silica. At present, it is difficult to determine whether, and under what conditions, complexation or electrostatics have a greater effect on metal hydroxide nucleation. Certainly, electrostatics impart a large influence on nucleation and are exerted under most conditions (i.e., even variable charged surfaces maintain some charge under most conditions due to the protonation reactions of different surface functional groups).

The sorption of Cr(III) on silica was influenced only by the degree of surface coverage; the pH and metal concentrations affected the nucleation structure in so much as they influence the amount of sorption (surface coverage). However this may not be the case in all reaction systems. If polymerization occurs in solution, often these species will preferentially adsorb due to their greater charge. Under such conditions, the metal ion concentration will have a dramatic influence on the sorption mechanism. Thus, sample preparation is a critical step for obtaining meaningful information. One should carefully evaluate the procedures employed to create an experimental system because often the results may be specific to those reaction conditions (experimental artifacts) rather than representing environmentally realistic situations.

Conclusions

The sorption mechanism of Cr(III) on silica differs from that on α-FeOOH or δ-MnO_2. Chromium(III) initially sorbs in a monodentate complex on silica. However, at greater than 20% surface coverage, the bridging of the sorbed species occurs. Rather than distributing over the silica surface, as results on α-FeOOH, the nucleation progresses away from the silica surface—out into the surrounding solution. The silica appears to impart structural constraints on the epitaxial growth of chromium hydroxide that are not energetically favorable. This results in the higher energy strained structure at the Cr–Si interface, and consequently nucleation progresses away from the silica surface, allowing for an unstrained γ-CrOOH type structure to develop.

At low surface coverage, adsorption appears to dominate the retention process. With increased Cr levels, polymerization of chromium hydroxide occurred, forming distinct entities on the surface. Further increases in Cr loadings on silica led to surface clustering. When the structures of the sorbent and sorbate are dissimilar, such as with Cr and silica, epitaxial growth appears to be energetically unfavorable, and the nucleation growth progressed away from the surface, i.e., the formation of surface clusters. However, on goethite, chromium hydroxide polymerization was observed to progress over the surface due to similar interatomic distances of the sorbent and sorbate [i.e., the O(H)–O(H) distances of the surface are similar to those of the chromium hydroxide].

In short, the predominant factors influencing the sorption mechanism of Cr(III) on oxides are the degree of surface coverage and the type of surface. Solution pH and Cr(III) concentration played a major role in determining the amount of sorption. Therefore, they affected the sorption mechanism indirectly by influencing the degree of surface coverage. Chromium concentrations appeared to influence the sorption mechanism by determining the amount of surface coverage.

Literature Cited

(1) Bleam, W. F.; McBride, M. B. *J. Colloid Interface Sci.* **1986**, *110*, 335.

(2) Charlet, L.; Manceau, A. *J. Colloid Interface Sci.* **1992**, *148*, 443.

(3) Chisholm-Brause, C. J.; O'Day, P. A.; Brown, G. E., Jr.; Parks, G. A. *Nature* **1990**, *348*, 528.

(4) Chisholm-Brause, C. J.; Row, A. L.; Hayes, K. F.; Brown, G. E., Jr.; Parks, G. A.; Leckie, J. O. *Geochim. Cosmochim. Acta* **1990**, *54*, 1897.

(5) Fendorf, S. E.; Fendorf, M.; Sparks, D. L.; Gronsky, R. *J. Colloid Interface Sci.* **1992**, *148*, 36.

(6) Manceau, A.; Charlet, L. *J. Colloid Interface Sci.* **1992**, *148*, 425.

(7) McBride, M. B. *Clays Clay Miner.* **1982**, *30*, 21.
(8) McBride, M. B.; Fraser, A. R.; McHardy, W. J. *Clays Clay Miner.* **1984**, *32*, 12.
(9) Schindler, P. W.; Stumm, W. In *Aquatic surface chemistry*; Stumm, W., Ed.; Wiley and Sons: New York, 1987; pp 83–110.
(10) Fendorf, S. E.; Lamble, G. M.; Stapleton, M. G.; Kelley, M. J.; Sparks, D. L. *Environ Sci. Technol.* **1994**, preceding paper in this issue.
(11) Fouad, N. E.; Knozinger, H.; Zaki, M. I.; Mansour, A. A. *Z. Phys. Chem. (Munich)* **1991**, *171*, 75.
(12) Allison, J.; Brown, D. S.; Nova-Gradac, K. J. *MINTEQA2/PRODEFA2, A geochemical assessment model for environmental systems: Version 3.0*; U.S. Environmental Protection Agency: Athens, GA, 1990.
(13) Rai, D.; Sass, B. M.; Moore, D. A. *Inorg. Chem.* **1987**, *26*, 345.
(14) Ryskin, Y. I. In *The infrared spectra of minerals*; Farmer, V. C., Ed.; Mineralogical Society: London, 1974; pp 137–181.
(15) Snyder, R. G.; Ibers, J. A. O-H-O and O-D-O potential energy curves for chromous acid. *J. Chem. Phys.* **1962**, *36*, 1356.
(16) Wyckoff, R. W. G. *Crystal Structures*; Interscience Publishing: New York, 1963.

Received for review April 19, 1993. Revised manuscript received September 10, 1993. Accepted October 20, 1993.[⊗]

[⊗] Abstract published in *Advance ACS Abstracts*, December 1, 1993.